

---

## The effect of heterogeneity in measles vaccination on population immunity

---

K. GLASS<sup>1</sup>\*, J. KAPPEY<sup>2</sup> AND B. T. GRENFELL<sup>2</sup>

<sup>1</sup> *National Centre for Epidemiology and Population Health, Australian National University, Canberra 0200, Australia*

<sup>2</sup> *Department of Zoology, University of Cambridge, Downing St, Cambridge CB2 3EJ, UK*

(Accepted 25 November 2003)

### SUMMARY

High overall vaccination levels sometimes hide pockets of poor coverage. We adopted a meta-population framework to model local aggregation of populations, and used this to investigate the effects of vaccination heterogeneity. A recent survey of antibody levels in a community with low vaccination levels in The Netherlands enabled us to assess the relative importance of local and long-range infective contacts, and thus identify feasible levels of aggregation in the meta-population model. In the aggregated model, we found that heterogeneity in vaccination coverage can lead to a much increased rate of infection among unvaccinated individuals, with a simultaneous drop in the average age at infection.

### INTRODUCTION

When protecting populations from disease, immunization policies aim for high national levels of coverage [1]. Often, a high overall vaccination level can mask a low coverage in certain regions [2–4]. Communities with low vaccination levels can then experience dramatic outbreaks [5] in contrast to that witnessed in well-vaccinated communities. Although it has been shown that carefully targeted heterogeneous vaccination policies can be advantageous [1, 6], the effect of intrinsic heterogeneity in vaccine coverage has been less studied. In the context of the current WHO initiative to eradicate measles in Europe by 2007 [7], an understanding of the impact of aggregation of susceptibles on levels of infection is highly important.

A series of continuous-time models based on the SIR (Susceptible–Infective–Recovered) framework have successfully captured both the recurrent pre-vaccination dynamics of measles epidemics and the impact of vaccination [1, 8, 9]. Recently, there has

been increasing focus on the population implications of waning of immunity [10–12]. In particular, we have developed an antibody model to describe both waning and boosting of immunity, and applied it to investigate the decrease in virus circulation that accompanies the onset of mass vaccination [13]. In a spatial context, the changes following the onset of vaccination are further complicated by spatial heterogeneity in vaccine uptake. We address that issue in this paper.

In order to model variability in local measles vaccination coverage, we adopted meta-population model. The meta-population framework is a well-established concept in population ecology [14, 15] that is increasingly being applied in epidemiology [16–18]. It allowed us to split a large population into a collection of local communities or patches. We inserted a disease transmission model into this framework, and could then specify the fraction of each individual's infectious contacts that must occur within the local community. Throughout this paper, we refer to the local communities as ‘patches’, and the fraction of infectious contacts that occur within the patch as the

\* Author for correspondence.

‘aggregation parameter’. We refer to populations with a large number of local contacts as being ‘highly aggregated’.

Meta-populations have been used to model measles transmission at a number of different scales. One obvious application of the meta-population model is to split a country into its many cities. At this scale, the size of a city is extremely important for determining persistence of disease [16, 19], demonstrating the importance of mixing within cities. Conversely, analysis of spread of infection indicates that mixing between cities occurs rapidly [20]. An examination of the epidemic correlations between regions in England and Wales shows a complex urban–rural pattern in the pre-vaccination era [21], and a drop in the correlation of epidemics between major cities after the introduction of vaccination [22]. The strong seasonal forcing of epidemics associated with schooling is also a complicating factor in the interpretation of correlations [20, 23]. At a much smaller scale, mathematical analysis of meta-populations of households has shown that both the epidemic threshold [24] and the critical immunization coverage [25] differ considerably from that of a homogeneously mixing population. In this paper, we consider mixing rates at an intermediate scale, similar to the resolution adopted by Bartlett [26]. Here, our meta-population represents a large city or municipality, and each patch represents a school and its local community.

One approach to modelling spatial heterogeneity of measles is the lattice-based model [26–29], where mixing rates are determined by relative positions in the lattice. Here, we do not impose any explicit spatial structure on the meta-population, but rather assume that local mixing leads to a greater risk of transmission within the local patch. In this way, the level of aggregation in the meta-population can be varied using a single ‘aggregation parameter’. The remaining difficulty lies in estimating the value of this parameter, as it incorporates demographic information on rates of mixing and movement that are extremely difficult to measure.

In modelling measles dynamics post-vaccination, it is important to consider both loss of vaccine-induced immunity, and boosting of immunity on contact with infection. We incorporated a previously developed measles antibody model [13] into the meta-population framework, which models the immune dynamics of the population. By applying this model, we were able to measure levels of immunity in different patches of the meta-population, and compare these model

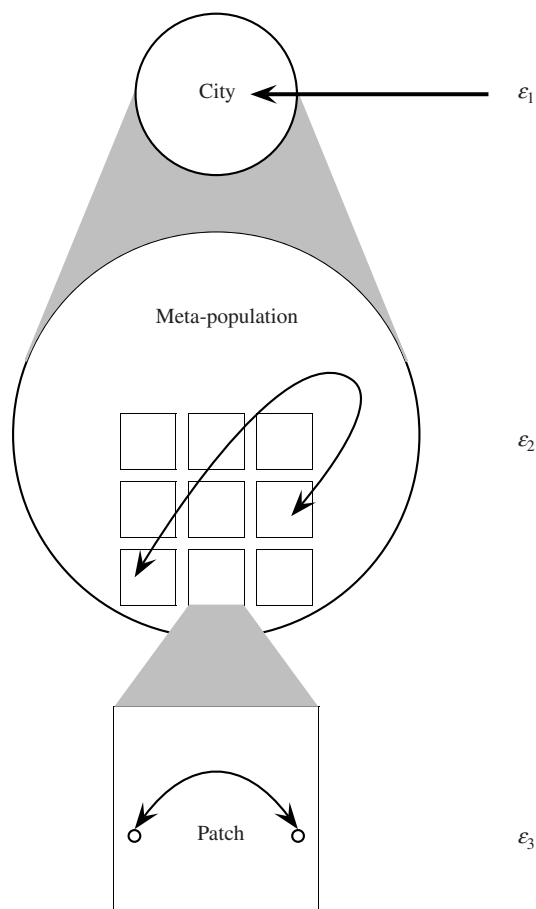


**Fig. 1.** Diagram representing the meta-population model on  $N$  patches of size  $M$ . The parameters determining the degree of isolation and aggregation are  $\epsilon_1$ ,  $\epsilon_2$  and  $\epsilon_3$  with  $\epsilon_1 + \epsilon_2 + \epsilon_3 = 1$  to ensure that  $R_0$  remains constant throughout. The unaggregated case corresponds to  $\epsilon_3 = 0$ , and the patches become completely isolated from one another if  $\epsilon_2 = 0$ .

predictions with data. A recent sample of antibody levels in The Netherlands found significant differences between groups with high- and low-vaccine coverage within the same municipality [4]. Comparison of model simulations with data allowed us to obtain bounds on the aggregation parameter, and then use these values in turn to simulate the effect of vaccine heterogeneity of disease incidence.

## METHODS

### The meta-population model

We adopted a simple meta-population model consisting of  $N$  patches of size  $M$  as shown in Figure 1. As measles infection largely occurs in children, we identified patches with the local community surrounding

a school, so that the meta-population as a whole forms a large city or municipality. Each individual in the meta-population has a fraction

- $\varepsilon_1$  of contacts with individuals outside the meta-population;
- $\varepsilon_2$  of contacts with randomly chosen individuals within the meta-population;
- $\varepsilon_3$  of contacts with individuals within the patch;

where  $\varepsilon_1$ ,  $\varepsilon_2$  and  $\varepsilon_3$  sum to 1. We assumed that there is a reservoir of infection outside the meta-population that can enter via parameter  $\varepsilon_1$ . This immigration term has little effect on the dynamics of large meta-populations, but is important for ensuring persistence when the population size is at or below the critical community size of 250 000–300 000 individuals [19]. A recent analysis [30] of mixing between populations is particularly relevant to this parameter, which is concerned with movement between cities. Within the meta-population, we assumed a slightly different mixing mechanism – rather than moving between school communities, we assumed that all individuals spend some fraction of their time in a general region (perhaps the town centre, local cinema or sports ground), where they can encounter any individual in the meta-population.

To simplify the number of parameters in the model, we assumed a fixed value for  $\varepsilon_1$  of 0.005, and a fixed patch size of 1000. The degree of aggregation is then completely determined by the aggregation parameter,  $\varepsilon_3$ . If  $\varepsilon_3 = 0$ , the meta-population becomes one homogeneously mixed population, and if  $\varepsilon_3 = 1 - \varepsilon_1 = 0.995$ , the patches become entirely disconnected from one another. The seasonality in contact rate induced by the school term is modelled by assuming that the transmission parameter varies annually as  $b(t)$ . The form of forcing function chosen (sinusoidal [31, 32] or term-time [8]) has little effect on the results; we adopted the former.

### The antibody model

A valuable opportunity for measuring the effects of population aggregation is provided by antibody data collected in areas with low vaccine coverage in The Netherlands [33]. Although national vaccination coverage is high (94%), there are a number of regions in which vaccination levels are low (62–84%) [4]. These low-vaccine communities (LVCs) contain geographically aggregated groups who refuse vaccination for religious reasons [33], and whose antibody

levels differ significantly from the national levels. A further distinction is made within the LVC by classifying individuals as either orthodox (who refuse vaccination) or non-orthodox.

In order to compare this antibody data with model simulations, we incorporated into the meta-population a modified version of a SIR model that includes immunity of individuals. The model is described in Figure 2, and further details may be found in [13]. Each individual in the model has an antibody level that is determined by that individual's prior infectious contacts. In the absence of infection, the antibody level decays exponentially to a limit value. On contact with infection, a vaccinated or recovered individual will become subclinically infected if their antibody level is below a threshold level, and this subclinical infection induces a boost to their antibody level. Susceptible individuals have an antibody level of zero, which is then raised to a maximum value by (clinical) infection. To ensure population heterogeneity, antibody levels are log-normally distributed about the mean values described by the antibody decay equations.

As discussed in [13] this model, with parameters assigned as in Figure 2, reproduces the national antibody-age profile seen in [4] very well. Figure 3*a* presents the national data, reproduced from [4], and Figure 3*b* the corresponding profile for a sample of 100 000 individuals from a simulation of 4 million. At the time that the antibody data were collected, vaccination had been in place for approximately 20 years. To reproduce the changes in immunity induced by the introduction of vaccination, the model is simulated for 100 years without vaccination, followed by 20 years with 90% vaccination. In Figure 3*c*, the comparison of data from the national and LVCs is reproduced from [4]. Individuals in the LVCs are identified as being either orthodox (light grey) or non-orthodox (dark grey). Observe that antibodies in the orthodox community are significantly lower than in both the national and non-orthodox samples for the 1–4 years age group, and significantly higher for age groups 10–14, 15–19 and 20–24 years. Significant differences between national and non-orthodox antibody levels can also be seen in the 1–9 years and 15–24 years age groups.

In our later simulations, we assumed a population size of 1 million. This is likely to be greater than the LVC municipalities surveyed in [4]. Although our simulations demonstrate the same broad results for smaller population sizes, the stochastic nature of the

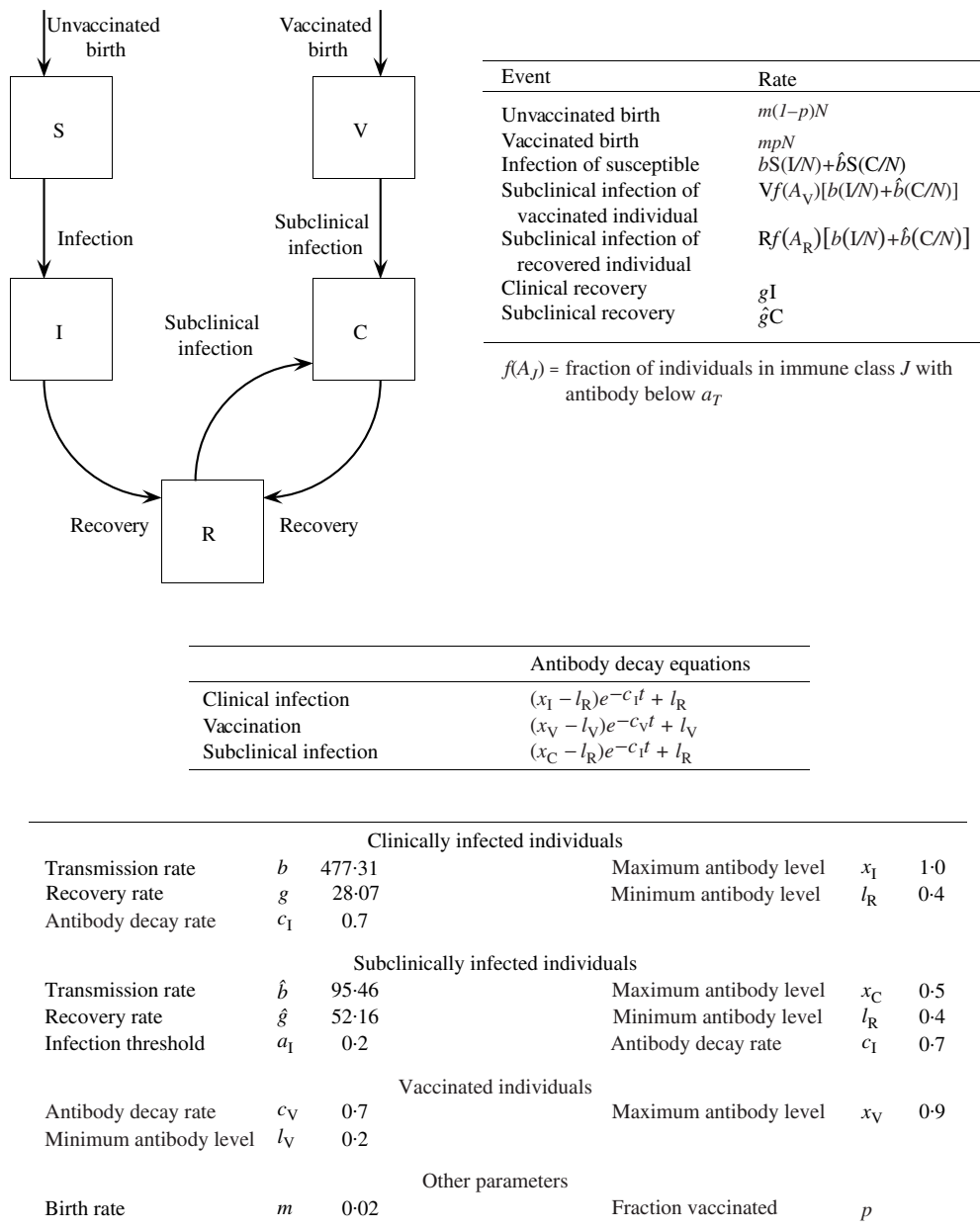


Fig. 2. Diagram, rates and parameters for the antibody model.

model leads to a fair degree of variability between replicates. We have chosen to present results from the model with a relatively large population, because this provides a more representative (and reproducible) picture of the typical behaviour of the model.

**RESULTS**

When modelling post-vaccination measles dynamics, it is important to include the effects of waning immunity and subclinical infection. By introducing the

antibody model (see Fig. 2) into the meta-population model, we were able to compare levels of immunity in different patches of the meta-population. Surveys of vaccination coverage in LVCs in The Netherlands estimated coverage within the orthodox community of 44% and within the non-orthodox community of 96%, while overall vaccination levels ranged from 62 to 84% [4]. We used our model to simulate a LVC with an overall average of 62% vaccination, split into 650 ‘orthodox’ patches with low vaccination (44%) and 350 ‘non-orthodox’ patches with high vaccination (96%). We expected that the significant

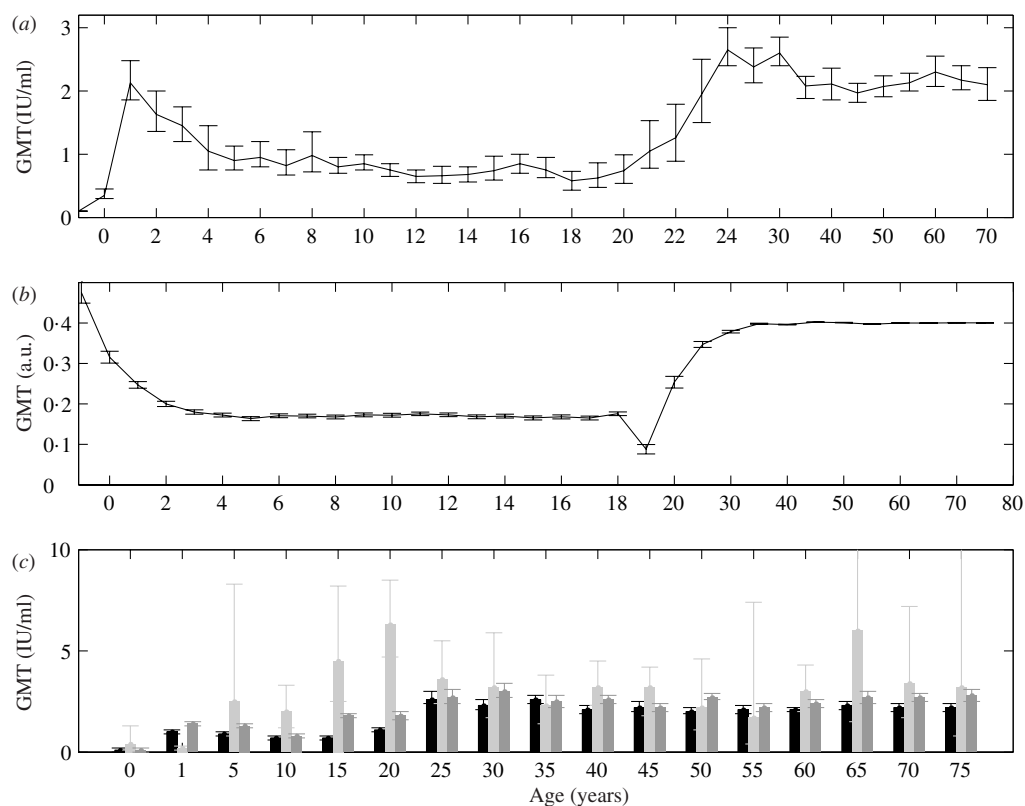


**Fig. 3.** Comparison of the antibody model (*b*) with data reproduced from [4] [*a*] and (*c*)]. Panel (*a*) gives the geometric mean titre with age for the national sample, and panel (*c*) compares the national sample (black) with samples from an area with low vaccine coverage, where individuals are further split into orthodox (light grey) and non-orthodox (dark grey) communities. Panel (*b*) gives the antibody-age profile of 100 000 individuals from a simulation of 4000 patches of size 1000, 20 years after introducing vaccination. For each figure, error bars give the 95% confidence interval for the mean. Note that while the units in (*a*) and (*c*) are IU/ml, the simulations use a dimensionless measure, calibrated by the parameters in Figure 2.

differences between the two communities to be in individuals below the age of 25 years, as the older individuals would be expected to have had measles before the onset of vaccination. When we compared the output of the model with the data collected in The Netherlands, we found that the age group most sensitive to changes in aggregation is the 10–14 years group. Figure 4 compares the data with the model simulations for increasing values of the aggregation parameter ( $\epsilon_3$ ). We see that without aggregation, the orthodox community has significantly lower antibody levels than that of the non-orthodox community – entirely the reverse of the data.

As the aggregation increases, unvaccinated orthodox individuals become more likely to be infected, and their overall geometric mean titre increases. Meanwhile, non-orthodox individuals become better protected from both clinical and subclinical infection, and their titres decrease. For  $\epsilon_3 \geq 0.5$ , the model reproduces the pattern of the data, and all significant

differences between the various communities identified in the other age groups.

Our results suggest that significant levels of aggregation are required to explain the high antibody levels in areas of low vaccine coverage. Within this context, patchiness in vaccination uptake can have a noticeable effect on infection dynamics, as susceptibles become grouped together. We test the effect of increasing the discrepancy between high- and low-vaccine regions in a meta-population with a fixed overall vaccination level, and a fixed level of local contacts. Figure 5 gives the results of simulations of 1000 patches of size 1000 for a population with 90% vaccination and  $\epsilon_3 = 0.6$  with increasing heterogeneity of vaccination.

In all plots, values for each of the 1000 patches are represented by dots, while the overall average for the meta-population is shown with an asterisk. Thus, the first panel shows the manipulation of vaccination coverage performed in the simulation. When heterogeneity (*h*) is at 0, all patches have 90% vaccination.

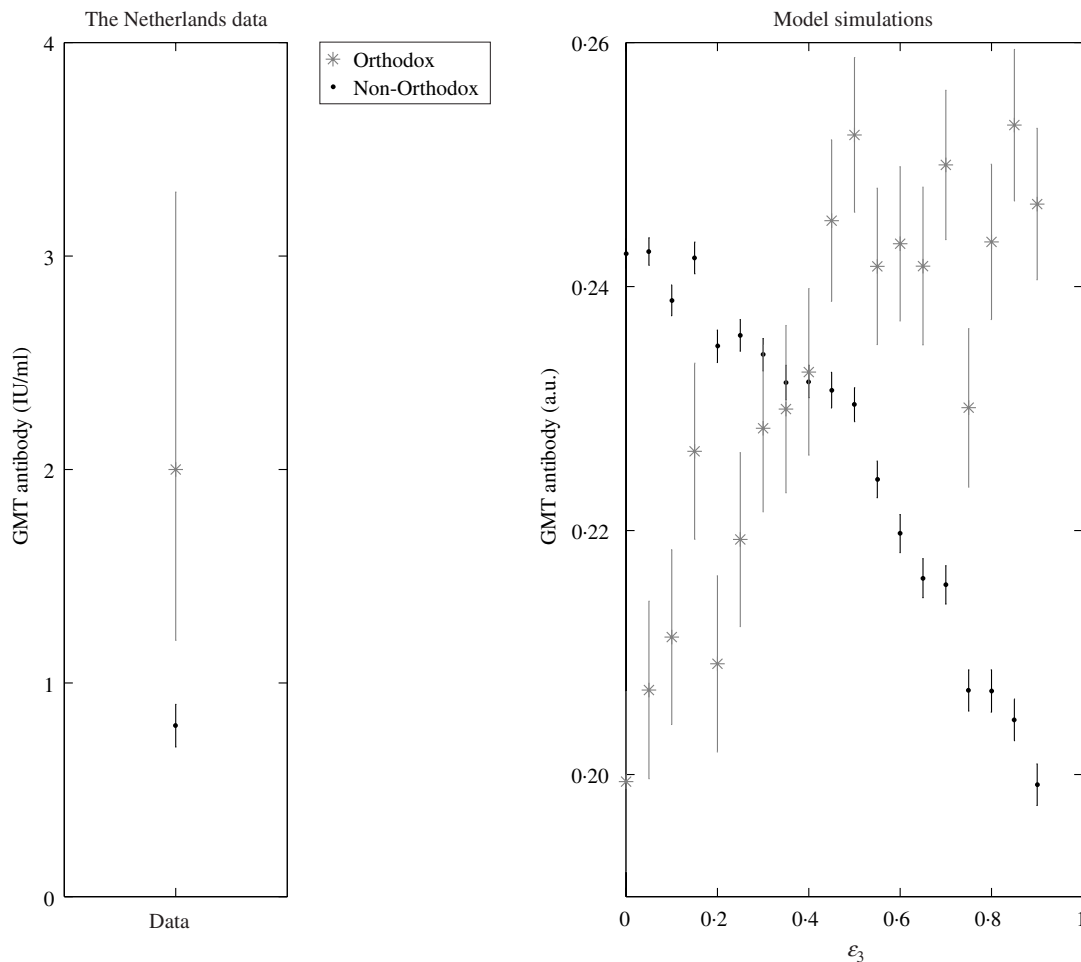


**Fig. 4.** Antibody levels of 10–14 years old orthodox and non-orthodox individuals in the low-vaccine community from [4], compared with output of the meta-population model with increasing level of aggregation (represented by the parameter  $\varepsilon_3$ ). For each plot, the error bars give the 95 % confidence interval for the mean. The antibody scale for the data is IU/ml, while the model uses a dimensionless scale described by the parameters in Figure 2.

As  $h$  is increased, vaccination decreases in 100 of the patches, and increases in the remaining 900 to maintain the overall vaccination at 90 %.

We see from Figure 5 that increased heterogeneity in vaccination leads to an overall increase in the risk of infection. In the model with homogeneous vaccination, on average 50 % of susceptibles are infected, with individual patches ranging from 40 to 60 %. As  $h$  increases, individuals in patches of low vaccination coverage become increasingly likely to become infected. We do see a simultaneous drop in the probability of infection of susceptibles in high vaccination areas, but as these susceptibles represent a decreasing fraction of the total susceptible population, this does not counteract the overall trend. A consequence of the increase in infection is a decrease in the average age at infection, led by the low-vaccination patches.

The rise in frequency of fadeouts suggests that outbreaks become more sporadic and thus also more dramatic.

## DISCUSSION

Standard models of measles transmission within urban communities assume that individuals mix homogeneously, even at population sizes in which some degree of aggregation of contacts must occur. Nevertheless, these models have been remarkably successful in reproducing measles dynamics, particularly the pre-vaccination time-series [34–36]. Our results suggest that this is because moderate levels of aggregation have only a small effect on the dynamical properties of measles in the pre-vaccination era, or when vaccination is homogeneous.

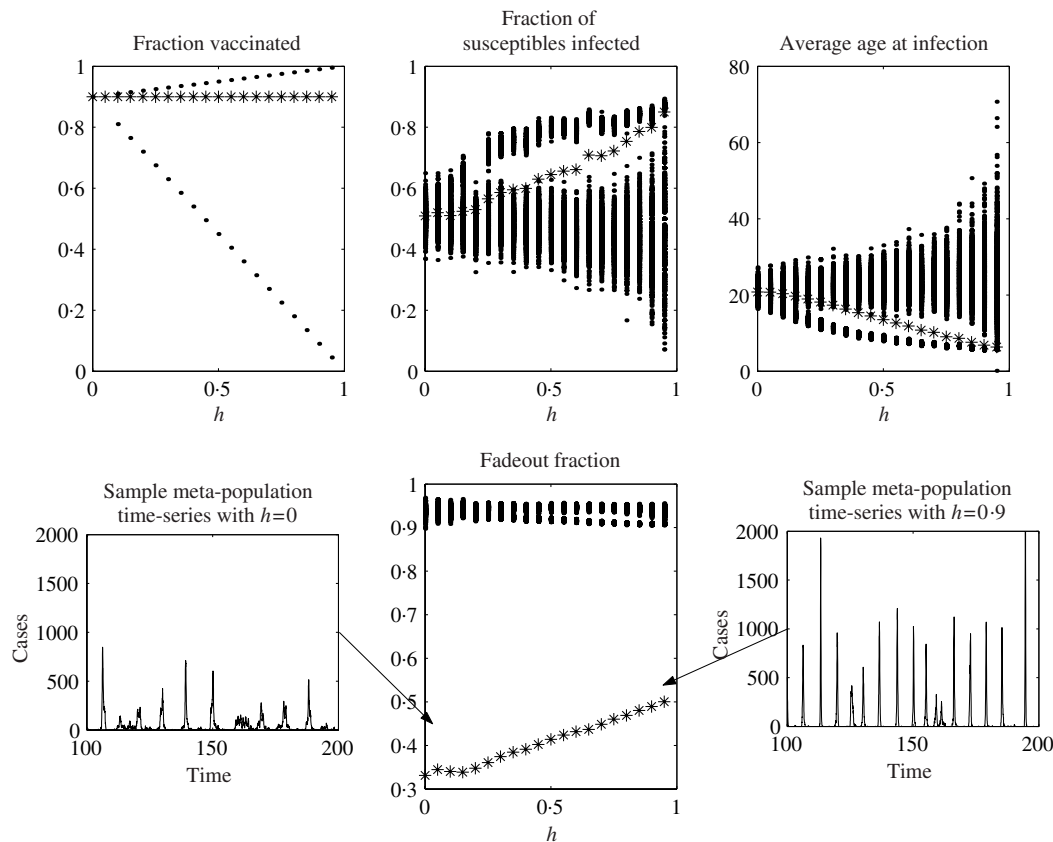


**Fig. 5.** Diagrams based on simulations of 1000 patches of size 1000 with fixed value of the aggregation parameter ( $\varepsilon_3 = 0.6$ ) and average of 90% vaccination. We vary the degree of heterogeneity ( $h$ ) in vaccination (as seen in the first panel), with 10% of patches at a low vaccination level, and the remaining patches at a higher level. For each plot, values for each of the 1000 patches are shown by a dot, and the value for the meta-population as a whole is shown by an asterisk. We also include a sample time-series for the meta-population for  $h=0$  and  $h=0.9$ . Fadeout is measured as the fraction of fortnights in which there were no new cases.

The situation changes when vaccination becomes patchy – low vaccine areas become infection hot-spots, with more dramatic outbreaks and a drop in the average age at infection. Data gathered from individuals in LVCs in The Netherlands [4] provides us with an opportunity to estimate the degree of aggregation present in these communities. We find that the antibody-age profiles can only be reproduced if we assume moderate to high levels of aggregation. Our model of immunity is very simple, assuming a single transmission rate between all age groups, and ignoring the effects of maternal immunity. Nevertheless it is able to reproduce all significant differences noted in The Netherlands data.

With the levels of aggregation estimated from the data, we then experiment with varying the patchiness in vaccination coverage within a hypothetical city with 1 million inhabitants, 10% of which are poorly vaccinated. We found that increasing vaccination

heterogeneity leads to an increase in the average fraction of susceptibles infected, from approximately 50 to 90% in a highly heterogeneous population. Standard models predict that vaccination of young children should significantly increase the mean age at infection of measles [1, 37, 38]. Our results indicate that strong spatial or social heterogeneity in vaccine uptake can mitigate this effect – we see a drop in the age at infection from  $\sim 20$  ( $h=0$ ) to  $\sim 6$  ( $h=0.95$ ). Clearly, the very high levels of heterogeneity represent an extreme case that is rarely seen, however the mean age at infection is reduced by even moderate levels of heterogeneity. These results are consistent with empirical findings – a recent outbreak of measles at an orthodox school in The Netherlands saw an attack rate of 91% among susceptibles, with 78% of the 138 cases occurring in children between the ages of 2 and 8 years [5]. It is clear that unvaccinated children face a much greater risk of infection when their

local community has a low vaccine coverage. Such LVCs face a constant danger of large outbreaks of infection, even when national levels of vaccination are high.

Throughout this paper, we have adopted the simplest form of meta-population model and ignored the effect of spatial structure. In future work we will look at models in which each patch mixes preferentially with its neighbours, and consider the effect that clustering of patches has on the meta-population dynamics.

## ACKNOWLEDGEMENTS

The authors thank Ottar Bjørnstad for useful discussions. Financial support was provided by the Wellcome Trust.

## REFERENCES

1. Anderson RM, May RM. Infectious diseases of humans: dynamics and control. Oxford University Press, 1991.
2. Hanratty BH, Holt T, Duffell E, et al. UK measles outbreak in non-immune anthroposophic communities: the implications for the elimination of measles from Europe. *Epidemiol Infect* 2000; **125**: 377–383.
3. Mossong J, Muller CP. Estimation of the basic reproduction number of measles during an outbreak in a partially vaccinated population. *Epidemiol Infect* 2000; **124**: 273–278.
4. van den Hof S, Berbers GAM, de Melker HE, Conyn van Spaendonck MAE. Sero-epidemiology of measles antibodies in the Netherlands, a cross-sectional study in a national sample and in communities with low vaccine coverage. *Vaccine* 2000; **18**: 931–940.
5. van den Hof S, Meffre CMA, Conyn van Spaendonck MAE, Woonink F, de Melker HE, van Binnendijk RS. Measles outbreak in a community with very low vaccine coverage, the Netherlands. *Emerg Infect Dis* 2001; **7**: 593–597.
6. May RM, Anderson RM. Spatial heterogeneity and the design of immunization programs. *Math Biosci* 1984; **72**: 83–111.
7. World Health Organisation. Strategies for reducing global measles mortality. *Wkly Epidemiol Rec* 2001; **75**: 411–416.
8. Schenzle D. An age-structured model of pre- and post-vaccination measles transmission. *IMA J Math Appl Med Biol* 1984; **1**: 169–191.
9. Earn DJD, Rohani P, Bolker BM, Grenfell BT. A simple model for complex dynamical transitions in epidemics. *Science* 2000; **287**: 667–670.
10. Davidkin I, Valle M. Vaccine-induced measles virus antibodies after two doses of combined measles, mumps and rubella vaccine: a 12-year follow-up in two cohorts. *Vaccine* 1998; **16**: 2052–2057.
11. Markowitz LE, Albrecht P, Orenstein WA, Lett SM, Pugliese TJ, Farrell D. Persistence of measles antibody after revaccination. *J Infect Dis* 1992; **166**: 205–208.
12. Mossong J, O’Callaghan CJ, Ratnam S. Modelling antibody response to measles vaccine and subsequent waning of immunity in a low exposure population. *Vaccine* 2001; **19**: 523–529.
13. Glass K, Grenfell BT. Antibody dynamics in childhood diseases: waning and boosting of immunity and the impact of vaccination. *J Theor Biol* 2003; **221**: 121–131.
14. Levins R. Some demographic and genetic consequences of environmental heterogeneity for biological control. *Bull Entomol Soc Am* 1969; **15**: 237–240.
15. Hanski I. Metapopulation dynamics. *Nature* 1998; **396**: 41–49.
16. Grenfell B, Harwood J. (Meta)population dynamics of infectious diseases. *Trends Ecol Evol* 1997; **12**: 395–399.
17. Lloyd AL, May RM. Spatial heterogeneity in epidemic models. *J Theor Biol* 1996; **179**: 1–11.
18. Keeling MJ. Metapopulation moments: coupling, stochasticity and persistence. *J Anim Ecol* 2000; **69**: 725–736.
19. Bartlett MS. The critical community size for measles in the United States. *J R Stat Soc A* 1960; **123**: 37–44.
20. Grenfell BT, Bjørnstad ON, Kappey J. Travelling waves and spatial hierarchies in measles epidemics. *Nature* 2001; **414**: 716–723.
21. Grenfell BT, Bolker BM. Cities and villages: infection hierarchies in a measles metapopulation. *Ecol Lett* 1998; **1**: 63–70.
22. Bolker BM, Grenfell BT. Impact of vaccination on the spatial correlation and persistence of measles dynamics. *Proc Natl Acad Sci USA* 1996; **93**: 12648–12653.
23. Bolker B, Grenfell B. Space, persistence and dynamics of measles epidemics. *Philos Trans Boil Sci* 1995; **348**: 309–320.
24. Ball F. Stochastic and deterministic models for SIS epidemics among a population partitioned into households. *Math Biosci* 1999; **156**: 41–67.
25. Becker NG, Utev S. The effect of community structure on the immunity coverage required to prevent epidemics. *Math Biosci* 1998; **147**: 23–39.
26. Bartlett MS. Measles periodicity and community size. *J R Stat Soc A* 1957; **120**: 48–70.
27. Kleczowski A, Grenfell BT. Mean-field equations for spread of epidemics: the ‘small world’ model. *Physica A* 1999; **274**: 355–360.
28. Rhodes CJ, Anderson RM. Persistence and dynamics in lattice models of epidemic spread. *J Theor Biol* 1996; **180**: 125–133.
29. Rhodes CJ, Anderson RM. Epidemic thresholds and vaccination in a lattice model of disease spread. *Theor Popul Biol* 1997; **52**: 101–118.
30. Keeling MJ, Rohani P. Estimating spatial coupling in epidemiological systems: a mechanistic approach. *Ecol Lett* 2002; **5**: 20–29.

31. London WP, Yorke JA. Recurrent outbreaks of measles, chickenpox and mumps. (I) Seasonal variation in contact rates. *Am J Epidemiol* 1973; **98**: 453–468.
32. London WP, Yorke JA. Recurrent outbreaks of measles, chickenpox and mumps. (II) Systematic differences in contact rates and stochastic effects. *Am J Epidemiol* 1973; **98**: 469–482.
33. De Melker HE, Conyn van Spaendonck MAE. Immunosurveillance and the evaluation of national immunization programmes: a population-based approach. *Epidemiol Infect* 1998; **121**: 637–643.
34. Bjørnstad ON, Finkenstädt BF, Grenfell BT. Dynamics of measles epidemics. (I) Estimating scaling of transmission rates using a time series SIR model. *Ecol Monogr* 2002; **72**: 169–184.
35. Grenfell BT, Bjørnstad ON, Finkenstädt BF. Dynamics of measles epidemics. (II) Scaling noise, determinism and predictability with the time series SIR model. *Ecol Monogr* 2002; **72**: 185–202.
36. Finkenstädt BF, Grenfell BT. Time series modelling of childhood diseases: a dynamical systems approach. *Appl Statist* 2000; **49**: 187–205.
37. Grenfell BT, Anderson RM. The estimation of age-related rates of infection from case notifications and serological data. *J Hyg Camb* 1985; **95**: 419–436.
38. Yang HM. Modeling directly transmitted infections in a routinely vaccinated population – the force of infection described by a Volterra integral equation. *Appl Math Comp* 2001; **122**: 27–58.